AQUA
Water Infrastructure, Ecosystems and Society

IWA PUBLISHING

 AQUA — Water Infrastructure, Ecosystems and Society Vol 71 No 1, 139 doi: 10.2166/aqua.2021.084

Design characteristics of showering aeration system

R. U. Roshan [a], Tanveer Mohammad [a,*], Subha M. Roy [b] and R. Rajendran [c]

[a] Department of Aquacultural Engineering, College of Fisheries Engineering, Tamil Nadu Dr J Jayalalithaa Fisheries University, Nagapattinam 611002, Tamil Nadu, India
[b] Agricultural Engineering Department, Triguna Sen School of Technology, Assam University, Silchar 788 011, Assam, India
[c] College of Fisheries Engineering, Tamil Nadu Dr J Jayalalithaa Fisheries University, Nagapattinam 611002, Tamil Nadu, India
*Corresponding author. E-mails: nobletanveer@gmail.com, mohammadtanveer@tnfu.ac.in

RUR, 0000-0002-2768-6327

ABSTRACT

The showering aeration system (SAS) was designed and its performance was evaluated by conducting the aeration experiments in a tank of dimension $2 \times 4 \times 1.5$ m. Initially, the aeration experiments were conducted to optimize the radius of curvature (r) of the SAS with different values, such as $r = 0$, 5, 10, 15, and 20 mm, and maintain other geometric parameters, i.e. number of holes in the shower (n); height of water fall (H); diameter of the shower hole (d); volume of water under aeration (V) and water flow rate (Q) as constants. The optimum radius of curvature (r) was found to be 10 mm. The aeration experiments were further conducted with four different non-dimensional geometric parameters such as the number of holes (n), the ratio of the height of water fall to the length of shower arm (H/l); the ratio of the diameter of the hole to the length of shower arm (d/l) and the ratio of the volume of water to the cube of the length of shower arm (V/l^3). The Response Surface Methodology and Box–Behnken Design were used to optimize the non-dimensional geometric parameters of the SAS to maximize the Non-Dimensional Standard Aeration Efficiency. The result indicates that the maximum NDSAE of 16.98×10^6 was obtained from the SAS performance at $n = 80$; $H/l = 2$; $d/l = 4$ and $V/l^3 = 48$.

Key words: aquaculture, non-dimensional geometric parameters, optimization, showering aeration system (SAS), standard aeration efficiency (SAE), water treatment

HIGHLIGHT

- The optimized non-dimensional geometric parameters (H/l; d/l; V/l^3; n) for the showering aeration system were experimentally validated, and the final NDSAE value was found to be 16.98×10^6 against the predicted NDSAE value of 17.70×10^6.

NOMENCLATURE

ANOVA	analysis of variance
θ	temperature correction factor
C	concentration of oxygen at time (ML^{-3})
C^*	oxygen saturation at standard conditions (ML^{-3})
C_0	dissolved oxygen concentration at time, $t = 0$ (ML^{-3})
DO	dissolved oxygen
Fr	Froude number
g	acceleration due to gravity (LT^{-2})
H	height of water fall (L)
K_La_{20}	standard oxygen transfer coefficient at 20 °C (T^{-1})
K_La_T	overall oxygen transfer coefficient at T°C (T^{-1})
n	number of holes in the shower
NDSAE	non-dimensional number characterizing SAE
P	power consumption (ML^2T^{-3})
Q	pump discharge/water flow rate (L^3T^{-1})
Re	Reynolds number
SOTR	standard oxygen transfer rate (MT^{-1})

SAE	standard aeration efficiency ($L^{-2}\,T^{2}$)
T	temperature (°C)
V	volume of water under aeration (L^{3})
W	Weber number
ρ_a	density of air (ML^{-3})
ρ_w	density of water (ML^{-3})
σ_w	surface tension of water (MT^{-2})
ν_w	kinematic viscosity of water ($L^{2}\,T^{-1}$)
RSM	Response Surface Methodology
SAS	showering aeration system
BBD	Box–Behnken Design
FCR	feed conversion ratio
SGR	specific growth rate
RGR	relative growth rate
r	radius of curvature (L)
D	distance between showers (L)
d	diameter of shower hole (L)
l	length of shower arm (L)

1. INTRODUCTION

Dissolved oxygen (DO) is one of the most vital parameters in the aquaculture water body, and it has a direct influence on aquatic lives. Therefore, it is essential to maintain the desired oxygen level in such water bodies through an artificial aeration system. An artificial aeration system is one of the methods of maintaining required DO levels in aquaculture ponds and water treatment plants (Roy *et al.* 2021a, 2021b, 2021c). The oxygen deficiency in the pond will retard the growth, locomotion, feeding, excretion and biosynthetic processes in the culture organisms (Van Dam & Pauly 1995). The minimum concentration of DO to be maintained is 5 mg/L and it is adequate for the aquatic organisms to respire. If DO level falls below 1–2 mg/L, it causes a high risk to the culture organism which even leads to mortality (Baylar *et al.* 2008; Boyd & Hanson 2010). Such risk factors can be avoided by facilitating the body of water with artificial aeration through mechanical aerating devices (Roy *et al.* 2015, 2017, 2020a, 2020b; Roy *et al.* 2022). Aerators enhance the interfacial area between the air and water, thus increasing the oxygen transfer rate, providing a better water circulation, and also preventing stratification of DO and temperature in the water body (Rogers 1989).

Different types of aeration devices have been developed to maintain desired levels of DO concentration in aquaculture operations in an effort to improve the aeration efficiency (Boyd 1998; Moulick *et al.* 2002, 2005, 2010; Roy *et al.* 2020a, 2022). The paddlewheel and the diffuser aeration systems are widely used in ponds and tank-based aquaculture systems, respectively. Ahmad & Boyd (1988) evaluated the performance of the paddle wheel aerator and found the Standard Aeration Efficiency (SAE) as 2.25 kgO_2/kWh. Roy *et al.* (2017) conducted a study in a different design of a paddle wheel aerator called a spiral aerator. The results showed that the maximum SAE is attained when the optimal number of handles per shaft and the rotational speed are 13 and 220 rpm, respectively. These aerators require significantly high energy input and also require constant maintenance, resulting in relatively higher running costs (Tanveer *et al.* 2018). Therefore, there is a need for a more environment-friendly, simple-to-operate, and economic aerator for aquaculture. It is firmly believed that the implementation of the SAS will reduce the cost of operation and maintenance while also potentially resolve the problems of low DO content, high concentration of volatile organic components, high accumulation of nitrogenous compounds and stratification.

The showering aeration system (SAS) is a splashing aerator that limits its usage to tank-based operations. A SAS consists of a required number of showers positioned in a horizontal pattern of polyvinyl chloride (UPVC) pipelines above the water surface to an average height of 1.0 m to distribute the water. The centrifugal pump is one of the primary components of SAS. It lifts the water to the desired height and it is dispersed into fine droplets of spray from the shower, which efficiently takes in oxygen from the atmosphere through adsorption. This flow creates a larger water surface area in contact with air, allowing the water to get oxygenated before falling into the tank (El-Zahaby & El-Gendy 2016). The efficiency of aeration depends on the surface area of the water droplet in contact with air, which is controlled primarily by the size of the shower opening and the dispersion of the water molecules. Studies suggest that the volume of water also influences the oxygen transfer rates. Elliott (1969) stated that the aerator power to water volume ratio should be less than 0.1 kW/m^3. These showers were designed and fabricated to enable the complete mixing of water in order to achieve DO destratification in the water column.

Studies were carried out in the area of showering aeration, which mainly focused on operating with a single shower in small capacity fiber-reinforced plastic (FRP) tanks. Salim *et al.* (2016) conducted the study with Nile tilapia in the SAS and obtained a satisfactory outcome in terms of feed conversion ratio, relative growth rate, specific growth rate and dissolved oxygen (DO) with the lowest energy consumption and higher net profit compared to the other aeration systems.

The present study attempted to develop a SAS with several showers in conjunction with a centrifugal pump as a primary aeration unit for usage in tank-based aquaculture and water treatment operations. The main features of the SAS are: it requires a small installation area, very minimum contact between the system and water, large specific area, thin film aeration, and requires minimum energy. It is believed that the implementation of such an aerator will reduce the cost of operation and manpower while also potentially resolving the problems in existing aeration systems like foam formation due to nutrient denaturation, clogging of nanopores in the aeration tubes, hypoxia and stratification. Therefore, in the present study, it was attempted to optimize the geometric parameters of SAS and evaluate its performance.

2. THEORETICAL ANALYSIS

The performance evaluation of aerators is mainly carried out in terms of standard oxygen transfer rate (SOTR) and the SAE.

The SOTR of an aeration system is defined as the mass of oxygen that the device can introduce into a body of water per unit time under standard circumstances of 20 °C water temperature, 0 mg/L initial DO concentration, one atmospheric pressure and clear tap water (APHA 1980; ASCE 1997).

$$\text{SOTR} = (k_L a)_{20} \times (C^* - C_0) \times V \tag{1}$$

where SOTR is the standard oxygen transfer rate (kgO_2/h), $(k_L a)_{20}$ is the standard oxygen transfer coefficient at 20 °C (h^{-1}), $(k_L a)_{20} = (k_L a)_T / \theta^{T-20}$, $(k_L a)_T$ is the overall oxygen transfer coefficient at T°C (h^{-1}), θ is the temperature correction factor of 1.024 for clean water, C^* is the saturation value of DO at test condition (mg/L), C_0 is the initial DO concentration (mg/L), V is the volume of water under aeration (m^3).

In most circumstances, larger aerators will transport more oxygen than smaller ones. So, the SAE, which is defined as the quantity of oxygen transported per unit of energy input, is a superior comparative parameter than SOTR (Lawson & Merry 1993). It is expressed as follows:

$$\text{SAE}(\text{kg } O_2/\text{kWh}) = \text{SOTR} \div P \tag{2}$$

where P is the power applied to the aerator (kW).

Power (P) in kW was estimated using the following equation:

$$P = (9.810 \times H \times Q) \div \eta \tag{3}$$

H = total head = static head + frictional head loss,
9.81 = acceleration due to gravity (m/s^2),
Q = flow rate (m^3/s), and
η = pump efficiency (42%).

2.1. Dimensional analysis

A laboratory-scale setup was used to conduct the aeration experiments. The results obtained from laboratory-scale experiments were interpreted and geometric dimensions were scaled up for the use of the aerator in an actual pond. The installation of SAS in the field requires a geometrical similarity condition, i.e., it should be built by following a definite geometric ratio with the corresponding dimensions of the laboratory-scale setup (Rao & Kumar 2007; Roy *et al.* 2020a, 2020b, 2021a, 2021b, 2021c). This geometric similarity is established with the corresponding dimensions of the laboratory system to achieve similar results of oxygen transfer rates in the field conditions. Generally, the oxygen transfer rate in water is determined by the size of the air bubbles and their distribution per unit volume. Also, the oxygen transfer rate is determined by

the physical characteristics of the water and air, flow parameters as well as the geometric parameters of the developed aeration system (Maise 1970). It may be categorized into three groups for convenience:

Geometric attributes: H = height of waterfall; n = number of holes in shower; l = length of shower arm; V = volume of water; d = diameter of the shower holes; D = distance between showers.
Process attributes: g = acceleration due to gravity; Q = discharge from the pump.
Material attributes: ρ_a = mass density of air; ρ_w = mass density of water; υ_w = kinematic viscosity; σ_w = surface tension of water.

The principal parameter of the absorption method is the absorption rate coefficient $(k_L a)_{20} \times V$ (Zlokarnik 1979). It is expressed as follows:

$$\mathrm{SOTR}/\Delta C = (k_L a)_{20} \times V \tag{4}$$

Therefore, the variables that affect the oxygen transfer rate at 20 °C can be expressed as the functional dependence of the aeration tank and the aeration system with a specific shape and design as follows:

$$\mathrm{SOTR}/\Delta C = f_1(H, n, l, V, d, D, \rho_a, \rho_{w,} g, Q, \upsilon_{w,} \sigma_w) \tag{5}$$

Lawson & Merry (1993) reported that SAE is a better comparative index than SOTR. So, SOTR is replaced by SAE. Also, the functional relation between SAE/ΔC and key variables can be expressed as follows:

$$\mathrm{SAE}/\Delta C = f_2(H, n, l, V, d, D, \rho_a, \rho_{w,} g, Q, \upsilon_{w,} \sigma_w) \tag{6}$$

Using the Buckingham's π theorem, l, ρ_w, g were chosen as the repeating variables and Equation (6) can be expressed as dimensionless as follows:

$$\text{Non-Dimensional SAE (NDSAE)} = \left\{\frac{H}{l},\ n,\ \frac{V}{l^3},\ \frac{d}{l},\ \frac{D}{l},\ \frac{\rho_a}{\rho_w},\ \frac{Q}{l^{\frac{5}{2}} \times \sqrt{g}},\ \frac{\upsilon_w}{l^{\frac{3}{2}} \times \sqrt{g}},\ \frac{\sigma_w}{l^2 \times \rho_w \times g}\right\} \tag{7}$$

where

$$\mathrm{NDSAE} = \frac{\mathrm{SAE}}{\Delta C} \times \frac{Q^2 \rho_w}{l^4}$$

$\frac{Q}{l^{\frac{5}{2}} \times \sqrt{g}}$ = Froude Number (Fr); (Roy *et al.* 2017, 2020a)
$\frac{\upsilon_w}{l^{\frac{3}{2}} \times \sqrt{g}}$ = Reynolds Number (Re); (Roy *et al.* 2017, 2020a)
$\frac{\sigma_w}{l^2 \times \rho_w \times g}$ = Weber Number (W).

Since the aeration tests were performed using only air and water, the ρ_a/ρ_w ratio remains the same in all the cases. The existing literature (Schmidtke & Horváth 1978; Rao 1999; Moulick *et al.* 2005; Moulick & Mal 2009; Kumar *et al.* 2013; Roy *et al.* 2015, 2017) shows that researchers needs to pay more attention to the Froude (Fr) and Reynolds (Re) numbers instead of Weber number (W) when evaluating the performance of aerators. Therefore, the Weber number (W) can be ignored and Equation (7) can be rewritten as follows:

$$\mathrm{NDSAE} = \left\{\frac{H}{l},\ n,\ \frac{V}{l^3},\ \frac{d}{l},\ \frac{D}{l},\ \mathrm{Fr},\ \mathrm{Re}\right\} \tag{8}$$

In the above formula, the first five dimensionless quantities determine the geometric similarity of the system, and the latter two dimensionless quantities determine the dynamic similarity. In the study, since the Froude (Fr) and Reynolds (Re) numbers are proportional to Q and inversely proportional to the length of shower arm (l) and distance between showers (D), so these variables are fixed as $Q = 0.0015\ \mathrm{m^3/s}$; $l = D = 0.5$ m.

3. MATERIALS AND METHODOLOGY

3.1. Experimental setup

A cemented concrete rectangular tank of dimensions $2 \times 4 \times 1.5$ m was used to evaluate the performance of the developed aeration system. A line sketch diagram of the aeration setup showing the sectional view (side and top views) is presented in Figure 1. The SAS was developed using various materials and fabricated as per the specifications furnished in Table 1. The system was operated with the centrifugal pump (1 HP), which was manufactured by Texmo Industries Pvt., Ltd. A control valve was provided to manage the flow of water, and the flow rate of water was measured using an electromagnetic flow meter. The system consists of the arrangement of pipes and showers at an average height of 1.0 m from the water surface. Initially, shower plates were designed and experiments were carried out to optimize the radius of curvature (r) (Figure 2). The radius of curvature (r) has a significant effect on the water spread area. The radius of curvature (r) at a particular point is defined as the radius of the approximating circle. After optimizing the radius of curvature (r), nine types of showers (8 nos. in each type) were fabricated with a combination of geometric parameters namely $n = 60$, 80, 100 and $d = 1.5$ mm, 2 mm, 2.5 mm as shown in Figure 3. The showers were assembled in an alternate pattern and are equally spaced as shown in the schematic diagram given below.

3.2. Aeration test

Unsteady state aeration tests were carried out in a concrete tank following the standard procedures with clean tap water (ASCE 1997). First, the tap water was deoxidized with 0.1 mg/L cobalt chloride and 10 mg/L sodium sulfite for each mg/L DO in the water (Boyd 1998). DO measurements were taken with YSI Professional 20 DO meters positioned at different points underneath the water surface (one at shallow depth and another at the middle of the water column). At least 20 DO measurements were carried out at equal time intervals till DO increases from 0% to 80% saturation (Baylar *et al.* 2007). After each measurement, the oxygen deficit (OD) or DO deficit was calculated. The oxygen transfer coefficient was determined using the slope of the best fit line obtained by graphing natural logarithms of DO deficits on the Y-axis against the period of aeration on the X-axis at the test water temperature. It is expressed as follows:

$$\text{Oxygen deficit (OD)} = C_s - C_m \tag{9}$$

$$(K_L a)T = (\ln \mathrm{OD}_{10} - \ln \mathrm{OD}_{80}) \div (t_{80} - t_{10}) \tag{10}$$

To compute SOTR, the oxygen transfer coefficient was adjusted to 20 °C using a temperature correction factor. It is given as follows:

$$(K_L a)_{20} = (K_L a)_T \div 1.024^{(T-20)} \tag{11}$$

Using the above values, SOTR and SAE can be computed with Equation (1).

3.3. Experimental design

3.3.1. Effect of the radius of curvature (r) of the shower plate of SAS on oxygen transfer

A series of preliminary trials were carried out to optimize the radius of curvature (r). Initially, five showers were fabricated with five different radiuses of curvature (r): 0, 5, 10, 15 and 20 mm. A testing setup was developed in an FRP tank of capacity 1 $\mathrm{m^3}$ to conduct the experiments. The operating parameters as well as the other geometric parameters and their values are given in Table 2. Aeration tests were performed with constant discharge, $Q = 0.0015\ \mathrm{m^3/s}$, to achieve a dynamic flow condition. In all the trials, the testing water was exchanged, deoxygenated, and then re-aerated according to the standard procedures (ASCE 1997) to compute the SAE.

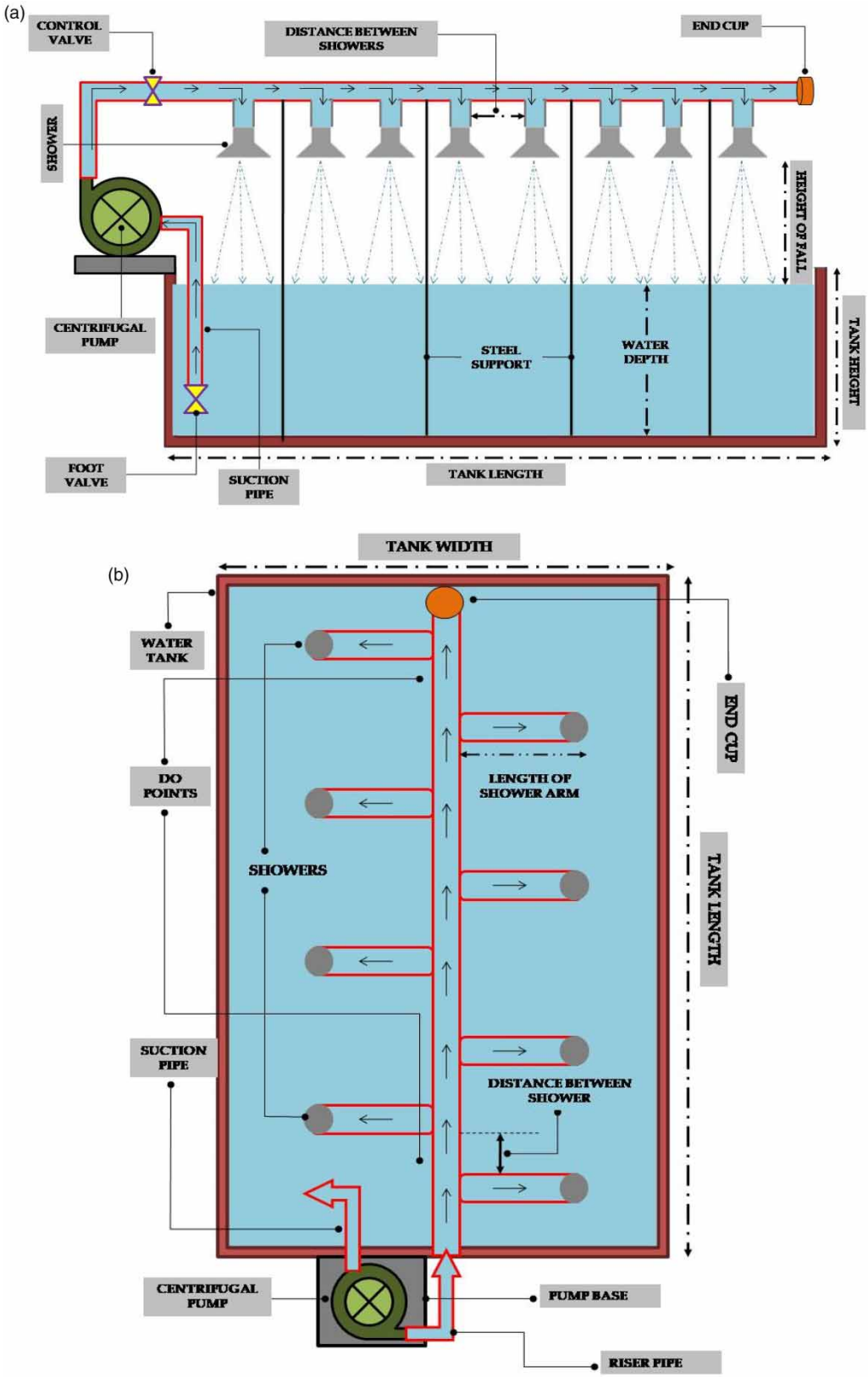

Figure 1 | (a) Side view and (b) top view of the schematic diagram of SAS.

Table 1 | Materials and specifications of the aerator

S. No.	Components	Raw materials
1	Showers	Made of SS 304
2	Support frame	Made of MS
3	Bolt and nut	Made of MS
4	Pipes	UPVC (1/4″)
5	Pump	One HP, three phase

3.3.2. Effect of the non-dimensional geometric ratios on oxygen transfer

For a specific dynamic condition (combined in the three parameters, Fr, Re and We), a particular set of values of the four non-dimensional geometric variables: the ratio of height of water fall to the length of shower arm (H/l); the ratio of diameter of shower holes to the length of shower arm (d/l); the ratio of volume of water to the cube of the length of the shower arm (V/l^3); the number of holes of the shower plate (n) that magnifies NDSAE can be found out. Hence, discharge (Q), radius of curvature (r) and distance between showers (D) were kept as a constant, which make Fr, Re and W invariants. A design of experiments based on Response Surface Methodology (RSM) was adopted considering H/l, d/l, V/l^3 and n as key variables. A Box–Behnken design (BBD) with six central points was used to develop the experimental design. The BBD was chosen for the evaluation because of its efficiency in terms of the number of runs necessary to find the second-order response surface model. The ranges of four independent variables $H/l = 1, 2, 3$; $d/l = 3, 4, 5$; $V/l^3 = 32, 40, 48$; $n = 60, 80, 100$ were selected on the basis of preliminary trials.

4. RESULTS AND DISCUSSION

4.1. Evaluation of radius of curvature (r) of the shower plate of SAS

Aeration experiments were carried on with five different radiuses of curvatures (r) = 0, 5, 10, 15, and 20 mm. A typical plot depicting the fluctuation of SAE with respect to r is shown in Figure 4.

$$\mathrm{SAE} = 0.56780 + (0.011020 \times r) - (0.000500 \times r^2)\ \{R^2 = 0.99\} \tag{12}$$

Differentiating the above equation,

$$\frac{d(\mathrm{SAE})}{d(n)} = 0.011020 - (0.001 \times r)$$

Assume, $\frac{d(\mathrm{SAE})}{d(n)} = 0$, we get $r = 11.02$–10 mm.

The maximum SAE was obtained at $r = 10$ mm. The SAE decreases as the radius of curvature (r) increases. This is because the water spreads out of the tank when r is higher. At the same time, when r is less than 10 mm, then there is no uniform distribution of the oxygenated water throughout the tank which eventually reduces the aeration efficiency.

4.2. Evaluation of optimum geometric parameters (H/l; d/l; V/l^3; n)

Further experiments were conducted under particular dynamic conditions and keeping the radius of curvature (r): 10 mm to determine the optimum non-dimensional geometric variables of the SAS. These experiments were designed using the RSM of BBD to study the effect of the four independent variables $H/l = 1, 2, 3$; $d/l = 3, 4, 5$; $V/l^3 = 32, 40, 48$; $n = 60, 80, 100$ on the NDSAE (Non-Dimensional SAE) of the SAS. The experimental results obtained are presented in Table 3. It is seen from Table 3 that the variation of NDSAE was from 7.597×10^6 to 15.914×10^6, and the corresponding SAE values are 0.6888 and 1.4429 $\mathrm{kgO_2/kWh}$, respectively.

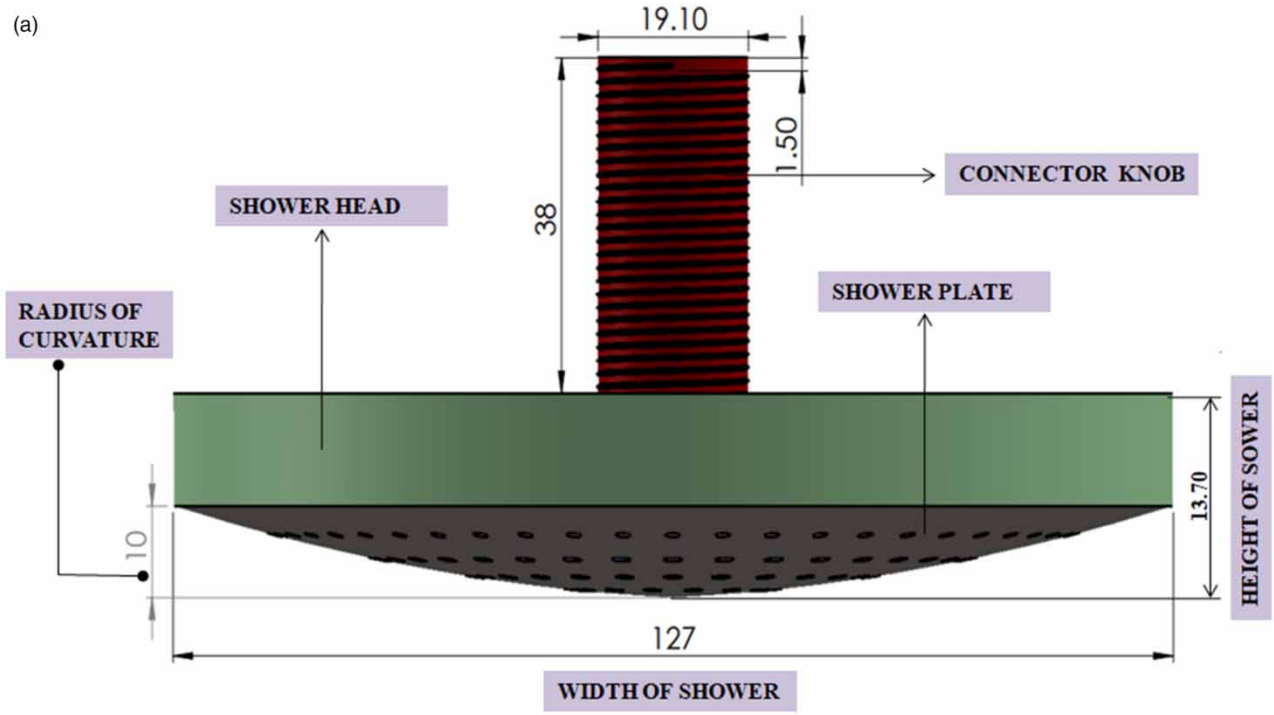

Figure 2 | (a) CAD model and (b) fabricated shower.

4.3. Model fitting and statistical analysis of the results

The experimental data were analyzed in Minitab 19 software using the RSM to determine the optimum geometric variables. From the analysis, it is obtained that a second-order polynomial (quadratic) was found to be fit.

$$\begin{aligned}\text{NDSAE} = {} & -85.7 + 1.530\,A + 10.39\,B + 22.61\,C - 0.985\,D - 0.008835\,A*A - 2.477\,B*B \\ & - 2.856\,C*C + 0.01516\,D*D + 0.00766\,A*B - 0.00755\,A*C - 0.00137\,A*D \\ & - 0.085\,B*C + 0.0018\,B* + 0.0062\,C*D\end{aligned} \tag{13}$$

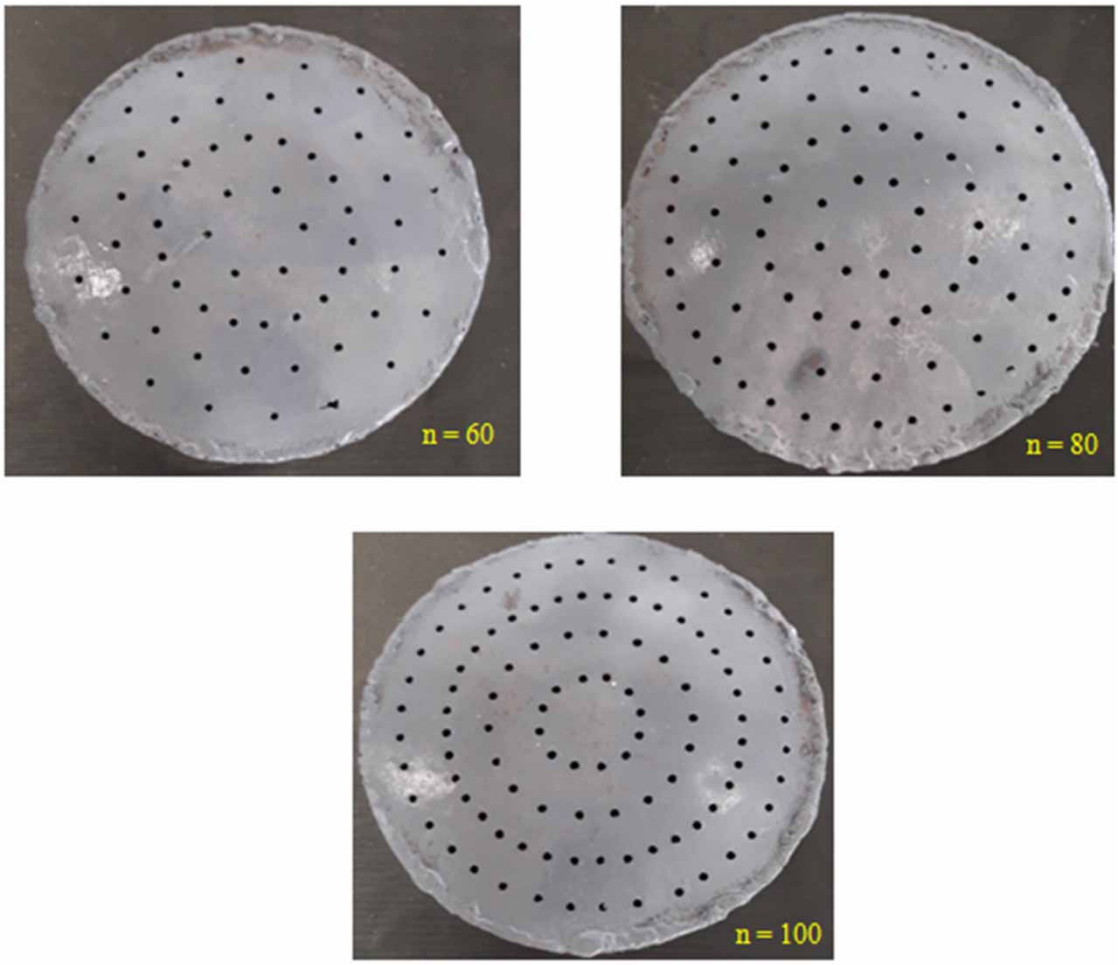

Figure 3 | Holes pattern of showers for different '*n*'.

Table 2 | Operating and constant parameters for the effect of radius of curvature (*r*)

	Varying geometric parameters		Constant geometric parameters	
S. No.	**Variable**	**Values (mm)**	**Variable**	**Values**
1	Radius of curvature (*r*)	0	*n*	80
2		5	*l*	0.5 m
3		10	*H*	1 m
4		15	*d*	2 mm
5		20	*V*	0.8 m^3

where A is the number of holes (n), B is the ratio of height of water fall to the length of shower arm (H/l), C is the ratio of diameter of holes to the length of shower arm (d/l), and D is the ratio of volume of water to the cube of the length of shower arm (V/l^3).

It is evident from Table 4 that the linear and quadratic models are highly significant with ($p < 0.05$) and the interactive models are not significant ($p > 0.05$). Therefore, the coefficient of the interactive model is withdrawn and the new regression

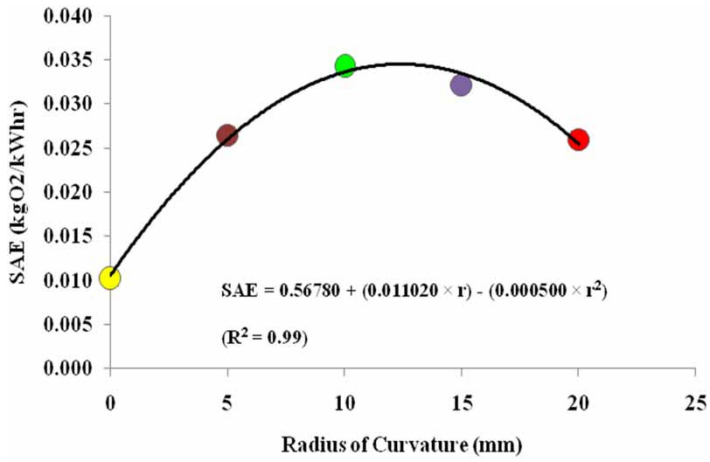

Figure 4 | Effect of radius of curvature (r) on SAE.

Table 3 | Experimental results of SAS for the optimization of (H/l; d/l; V/l^3; n)

Run	n	H/l	d/l	V/l^3	SOTR (kgO_2/h)	SAE (kgO_2/kWh)	NDSAE × 10^6
1	80	1	4	32	0.0554	1.1087	12.228
2	80	3	5	40	0.0554	1.1087	12.228
3	80	2	5	32	0.0537	1.0732	11.836
4	80	1	4	48	0.0660	1.3198	14.556
5	100	2	4	48	0.0677	1.3537	14.93
6	100	2	5	40	0.0425	0.8497	9.371
7	100	2	3	40	0.0501	1.0021	11.052
8	60	1	4	40	0.0359	0.7187	7.927
9	100	2	4	32	0.0584	1.1678	12.88
10	60	2	5	40	0.0344	0.6888	7.597
11	80	1	3	40	0.046	0.9196	10.142
12	80	2	4	40	0.0706	1.4123	15.576
13	80	2	5	48	0.0642	1.2834	14.155
14	80	3	4	48	0.0721	1.4429	15.914
15	60	2	4	32	0.0494	0.9873	10.889
16	80	1	5	40	0.0377	0.754	8.316
17	80	2	3	32	0.0595	1.1894	13.118
18	100	1	4	40	0.0437	0.8746	9.646
19	80	3	3	40	0.057	1.1399	12.572
20	60	3	4	40	0.0407	0.8132	8.969
21	60	2	4	48	0.0626	1.2525	13.814
22	60	2	3	40	0.0393	0.7865	8.674
23	80	2	3	48	0.0691	1.3816	15.238
24	80	3	4	32	0.0613	1.2265	13.527
25	100	3	4	40	0.0512	1.0247	11.301

Table 4 | ANOVA for NDSAE

Source	d.f.	Adj. SS	Adj. MS	*F*-Value	*P*-Value
Model	14	154.795	11.0568	83.51	0.000
Linear	4	42.344	10.5859	79.96	0.000
A	1	10.660	10.6597	80.51	0.000
B	1	8.125	8.1247	61.37	0.000
C	1	6.924	6.9236	52.29	0.000
D	1	16.636	16.6357	125.65	0.000
Square	4	112.035	28.0088	211.55	0.000
*A***A*	1	35.267	35.2668	266.37	0.000
*B***B*	1	17.330	17.3297	130.89	0.000
*C***C*	1	23.027	23.0274	173.93	0.000
*D***D*	1	2.658	2.6578	20.07	0.001
Two-way Interaction	6	0.416	0.0694	0.52	0.779
*A***B*	1	0.094	0.0939	0.71	0.419
*A***C*	1	0.091	0.0912	0.69	0.426
*A***D*	1	0.191	0.1914	1.45	0.257
*B***C*	1	0.029	0.0289	0.22	0.650
*B***D*	1	0.001	0.0009	0.01	0.937
*C***D*	1	0.010	0.0099	0.07	0.790
Error	10	1.324	0.1324		
Total	24	156.119			

@95% Confidence level of significance, $R^2 = 99\%$, R^2 (adjusted) = 97%.

equation was obtained to precisely describe the response surface of NDSAE (Equation (14)).

$$\begin{aligned}\text{NDSAE} = {} & -80.6 + 1.4608\,A + 10.733\,B + 22.09\,C - 1.066\,D - 0.008835A*A \\ & - 2.477\,B*B - 2.856\,C*C + 0.01516\,D*D\end{aligned} \tag{14}$$

where the coefficients are the same as for Equation (13).

The obtained quadratic equation implies that the model might be well fitted for the experimental design. The coefficient of regression (R^2) and *p*-values are 0.99 and 0.000, respectively. The ANOVA of the fitted model indicates that the regression is significant; hence, it is inferred that adequacy of the designed model is satisfactory for the experimental data (Montgomery 2017).

4.4. Effect of geometric parameters on NDSAE

The effects of the NDSAE over the four geometric variables are given in Figures 5–8, respectively.

NDSAE is linearly proportional to the number of holes (n) and reaches a maximum when $n = 80$, as shown in Figure 5. This is due to the fact that flow of water to fall vertically through the holes in the form of fine spray, which creates a large number of air bubbles in the water body. These air bubbles enhance the oxygen transfer, which finally increases the aeration efficiency. Following that, NDSAE begins to decline as n exceeds 80. This is due to the fact that as the number of holes increases, there is non-uniform distribution of water. This phenomenon decreases the air–water contact period and comparatively less oxygen transfer takes place, which finally reduces the NDSAE.

Figure 6 illustrates that, as the ratio of the height of the fall to the length of the shower arm (H/l) rises, NDSAE also increases simultaneously. This is because as the height of the fall increases, the water's residence time in the air increases (Navisa *et al.* 2014). The SAE, which corresponds to the maximum NDSAE, ultimately increases as a result of the increase in residence time. A higher range of aeration is attained at $H/l = 2$.

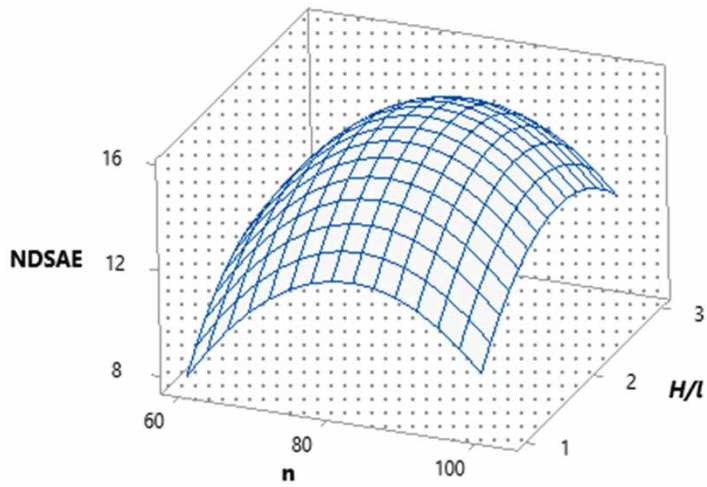

Figure 5 | Interactive effects of n and H/l.

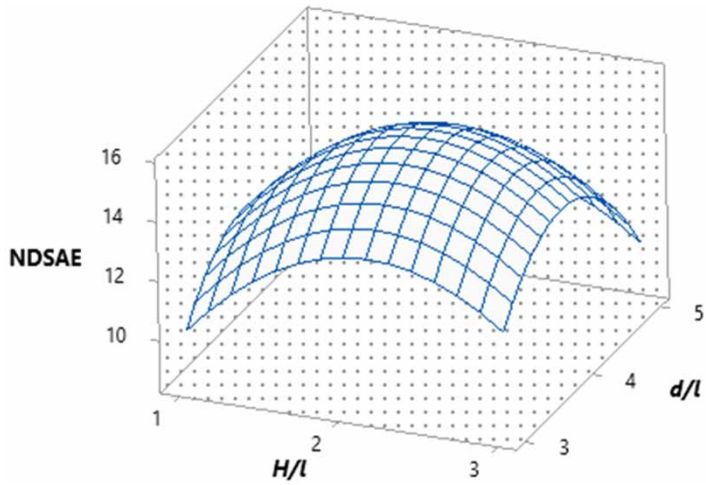

Figure 6 | Interactive effects of H/l and d/l.

Figure 7 illustrates that the ratio of volume to the cube of the length of shower arm (V/l^3) is directly proportional to NDSAE. The phenomenon behind the process is that when the water volume is higher, the oxygenated water has a longer residence time in the body of water and tends to mix and circulate for a longer period of time (Al-Ahmady 2006). This results in an increase in oxygen transfer that eventually elevates the levels of SAE and NDSAE as well.

Figure 8 interprets that initially the NDSAE increases with the ratio of diameter of the holes to the length of shower arm d/l and it also reaches its peak when $d/l = 4$. Beyond that the NDSAE progressively decreases as the d/l value increases. This is due to the fact that when the diameter of the pores increases, it may be unable to break down the water particles into smaller droplets, failing to create more air–water contact area resulting in improper oxygenation.

5. MODEL VALIDATION

The optimization of non-dimensional geometric variables was performed using 'Response optimization' in the Minitab 19 software. The obtained optimum values of non-dimensional geometric variables are listed in Table 5. Further, these geometric

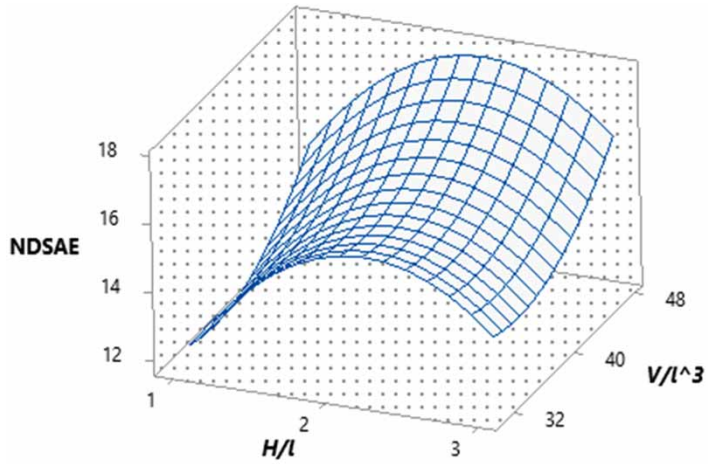

Figure 7 | Interactive effects of H/l and V/l^3.

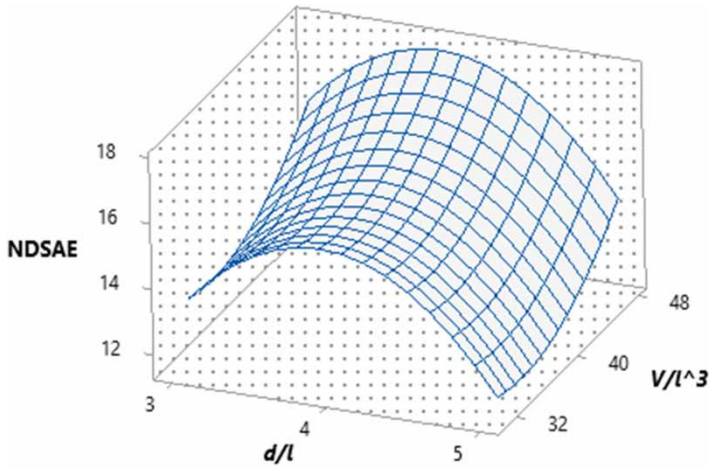

Figure 8 | Interactive effects of d/l and V/l^3.

Table 5 | Optimum values of geometric parameters of SAS

			Actual value	
Variable	**Optimum values**	**Predicted response value, NDSAE × 10^6**	**SAE (kgO_2/kW h)**	**NDSAE × 10^6**
n	80	17.70	1.54	16.98
H/l	2			
d/l	4			
V/l^3	48			

parameters were validated to re-assess the designed model, and the predicted and experimental results are given in Table 5. The predicted and experimented values of NDSAE were nearly similar with the standard deviation of ± 0.51. Hence, the result of the model validation was satisfactory and thus justifying the adequacy of the model.

6. SUMMARY AND CONCLUSION

The current study investigates how the different geometric factors affect the aeration characteristics of the SAS. The geometric variables were optimized in order to improve the efficiency of the SAS. The maximum SAE and NDSAE obtained from experimental trials were 1.4429 kgO_2/kWh and 15.914×10^6, respectively. To determine the optimum geometric parameters, the experimental results were validated using the RSM.

The major conclusions drawn from the obtained results are as follows:

1. The optimum radius of curvature (r) should be 10 mm to attain maximum SAE that corresponds to the maximum NDSAE.
2. Response surface graphs can be used to describe the effect of the geometric variables on the performance of the SAS.
3. For achieving the maximum NDSAE, H/l, d/l, V/l^3 and n are 2, 4, 48 and 80, respectively.
4. The predicted NDSAE and SAE values obtained from the developed model at the optimum geometric variables were found to be 17.70×10^6 and 1.54 kgO_2/kWh, respectively.
5. The optimized non-dimensional geometric parameters (H/l; d/l; V/l^3; n) for the SAS were experimentally validated, and the final NDSAE value was found to be 16.98×10^6 against the predicted NDSAE value of 17.70×10^6.

Finally, it may be said that the developed RSM/BBD model is an effective tool for predicting the optimized geometric variables of the SAS.

ACKNOWLEDGEMENT

The authors are thankful to the College of Fisheries Engineering, Tamil Nadu Dr J. Jayalalithaa Fisheries University for providing support and motivation to conduct the study.

DATA AVAILABILITY STATEMENT

All relevant data are included in the paper or its Supplementary Information.

REFERENCES

Ahmad, T. & Boyd, C. E. 1988 Design and performance of paddle wheel aerators. *Aquacultural Engineering* **7** (1), 39–62.

Al-Ahmady, K. K. 2006 Effect of airflow rate and submergence of diffusers on oxygen transfer capacity of diffused aeration systems. *Al-Rafidain Engineering Journal (AREJ)* **14** (1), 27–38.

American Society of Civil Engineers (ASCE) 1997 *Standard Guidelines for In-Process Oxygen Transfer Testing*. ASCE, New York, USA.

APHA 1980 *American Water Works Association and Pollution Control Federal*, 16th edn. APHA, Washington, DC, p. 1268.

Baylar, A., Hanbay, D. & Ozpolat, E. 2007 Modeling aeration efficiency of stepped cascades by using ANFIS. *CLEAN – Soil, Air, Water* **35** (2), 186–192.

Baylar, A., Hanbay, D. & Ozpolat, E. 2008 An expert system for predicting aeration performance of weirs by using ANFIS. *Expert Systems with Applications* **35** (3), 1214–1222.

Boyd, C. E. 1998 Pond water aeration systems. *Aquacultural Engineering* **18** (1), 9–40.

Boyd, C. E. & Hanson, T. 2010 Dissolved-oxygen concentrations in pond aquaculture. *Global Aquaculture Alliance* **13** (1), 40–41.

Elliott, J. W. 1969 The oxygen requirements of Chinook salmon. *The Progressive Fish-Culturist* **31** (2), 67–73.

El-Zahaby, A. M. & El-Gendy, A. S. 2016 Passive aeration of wastewater treated by an anaerobic process – adesign approach. *Journal of Environmental Chemical Engineering* **4** (4), 4565–4573.

Kumar, A., Moulick, S., Singh, B. K. & Mal, B. C. 2013 Design characteristics of pooled circular stepped cascade aeration system. *Aquacultural Engineering* **56**, 51–58.

Lawson, T. B. & Merry, G. E. 1993 Procedures for evaluating low-power surface aerators under field conditions. *Techniques for Modern Aquaculture*, p. 511.

Maise, G. 1970 Scaling methods for surface aerators. *Journal of the Sanitary Engineering Division* **96** (5), 1079–1083.

Montgomery, D. C. 2017 *Design and Analysis of Experiments*. John Wiley & Sons, New York.

Moulick, S. & Mal, B. C. 2009 Performance evaluation of double-hub paddle wheel aerator. *Journal of Environmental Engineering* **135** (7), 562–566.

Moulick, S., Mal, B. & Bandyopadhyay, S. 2002 Prediction of aeration performance of paddle wheel aerators. *Aquacultural Engineering* **25** (4), 217–237.

Moulick, S., Bandyopadhyay, S. & Mal, B. C. 2005 Design characteristics of single hub paddle wheel aerator. *Journal of Environmental Engineering* **131** (8), 1147–1154.

Moulick, S., Tambada, N. V., Singh, B. K. & Mal, B. C. 2010 Aeration characteristics of a rectangular stepped cascade system. *Water Science and Technology* **61** (2), 415–420.

Navisa, J., Sravya, T., Swetha, M. & Venkatesan, M. 2014 Effect of bubble size on aeration process. *Asian Journal of Scientific Research* **7** (4), 482.
Rao, A. R. 1999 Prediction of reaeration rates in square, stirred tanks. *Journal of Environmental Engineering* **125** (3), 215–223.
Rao, A. R. & Kumar, B. 2007 Neural modeling of square surface aerators. *Journal of Environmental Engineering* **133** (4), 411–418.
Rogers, G. L. 1989 Aeration and circulation for effective aquaculture pond management. *Aquacultural Engineering* **8** (5), 349–355.
Roy, S. M., Moulick, S., Mukherjee, C. K. & Mal, B. C. 2015 Effect of rotational speeds of paddle wheel aerator on aeration cost. *American Research Thoughts* **2** (1), 3069–3087.
Roy, S. M., Moulick, S. & Mal, B. C. 2017 Design characteristics of spiral aerator. *Journal of the World Aquaculture Society* **48** (6), 898–908.
Roy, S. M., Moulick, S. & Mukherjee, C. K. 2020a Design characteristics of perforated pooled circular stepped cascade aeration system. *Journal of Water Science & Technology – Water Supply* **20** (5), 1692–1705.
Roy, S. M., Tanveer, M., Mukherjee, C. K. & Mal, B. C. 2020b Design characteristics of perforated tray aerator. *Journal of Water Science & Technology – Water Supply* **20** (5), 1643–1652.
Roy, S. M., Jayraj, P., Machavaram, R., Pareek, C. M. & Mal, B. C. 2021a Diversified aeration facilities for effective aquaculture systems – a comprehensive review. *Aquaculture International* **29**, 1181–1217.
Roy, S. M., Gupta, D., Pareek, C. M., Tanveer, M. & Mal, B. C. 2021b Prediction of aeration efficiency of diffuser aerator using artificial neutral network and response surface methodology. *Journal of Water Science & Technology – Water Supply*. doi:10.2166/ws.2021.199.
Roy, S. M., Pareek, C. M., Machavaram, R. & Mukherjee, C. K. 2021c Optimizing the aeration performance of perforated pooled circular stepped cascade using hybrid ANN-PSO techniques. *Information Processing in Agriculture*. https://doi.org/10.1016/j.inpa.2020.04.005.
Roy, S. M., Machavaram, R., Moulick, S. & Mukherjee, C. K. 2022 Economic feasibility study of aerators in aquaculture using life cycle costing (LCC) approach. *Journal of Environmental Management* **302**, 114037. https://doi.org/10.1016/j.jenvman.2021.114037.
Salim, M. A., Tawfik, M. A., Abdallah, Y. S. & AboSaif, R. A. 2016 Effect of different aeration system on Nile Tilapia (OreochromisNiloticus) production. *Zagazig Journal of Agricultural Research* **43** (6), 2197–2213.
Schmidtke, N. W. & Horváth, I. 1978 Scale-up methodology for surface aerated reactors. In: S. H. Jenkins, ed. *Eighth International Conference on Water Pollution Research*. Pergamon, Sydney, pp. 477–493.
Tanveer, M., Roy, S. M., Vikneswaran, M., Renganathan, P. & Balasubramanian, S. 2018 Surface aeration systems for application in aquaculture: a review. *International Journal of Fisheries and Aquatic Studies* **6** (5), 342–347.
Van Dam, A. A. & Pauly, D. 1995 Simulation of the effects of oxygen on food consumption and growth of Nile tilapia, *Oreochromis niloticus* (L.). *Aquaculture Research* **26** (6), 427–440.
Zlokarnik, M. 1979 Scale-up of surface aerators for waste water treatment. In: T. Scheper, ed. *Advances in Biochemical Engineering, Volume 11*. Springer, Berlin, Heidelberg, pp. 157–180.

First received 6 July 2021; accepted in revised form 13 December 2021. Available online 29 December 2021